J. Plasma Physics (2015), *vol.* 81, 905810113 © Cambridge University Press 2014
doi:10.1017/S0022377814000543

Dynamic behavior of the (3+1)-dimensional generalized Johnson model in a dusty plasma

Hui-Ling Zhen, Bo Tian†, Wen-Rong Sun and Zhao Tan

State Key Laboratory of Information Photonics and Optical Communications, and School of Science, Beijing University of Posts and Telecommunications, Beijing 100876, China

(Received 8 April 2014; revised 24 June 2014; accepted 4 July 2014; first published online 11 August 2014)

In this paper, we study the (3+1)-dimensional generalized Johnson model, which can be used to describe the dust-ion-acoustic waves in a cosmic unmagnetized dusty plasma, and its perturbed model, which can be found in an unmagnetized dusty plasma for the electron temperature below the Curie temperature. (I) For the original model: Bilinear form and soliton solutions are obtained. Amplitude of the one soliton reaches the maximum when the equilibrium electron (n_{e0}) and ion (n_{i0}) densities take certain values which correspond with $n_{e0}/n_{i0} = 2$. Overtaking and head-on interactions between the two solitons are given. (II) For the perturbed model: Phase projections are given numerically. Via the spectral analysis, two kinds of chaotic motions, i.e., the weak and developed chaos, are investigated. Largest Lyapunov exponents and power spectra are investigated to corroborate that those motions are indeed chaotic. Dynamic behavior of such a perturbed model varying with the external perturbation is different when the nonlinear term changes. With the damped term considered, two kinds of periodic motions are studied, and spectra of those periodic motions are also given. Through the comparison between the chaotic motions and periodic ones, possible chaotic or periodic motions in the perturbed model can be predicted.

1. Introduction

Studies on the dynamics of dusty plasmas and their models have revealed the role of plasmas containing the heavy dust particles in different types of the collective processes in the cosmic and laboratory environments (Shukla 2001; Tsytovich et al. 2002; Shukla and Mamun 2002; Morfill et al. 2003; Fortov et al. 2005). Literatures have shown that the dust particles can affect the plasma environments and vary the collective behavior of the plasmas via inducing the new instabilities and altering the wave modes (Tian and Gao 2005a; Choi et al. 2005; Moslem 2006). Experiments and numerical calculations have both found that the presence of charged heavy dust particles in the plasmas not only affects the wave spectra of plasmas without the dust particles, but also introduces certain eigenmodes, such as the dust-acoustic waves and dust-ion-acoustic (DIA) waves (Sahu and Roychoudhury 2003; Pope et al. 2005; Duha et al. 2011; Tian and Gao 2005b).

Applications of the dusty-plasma interactions in the industrial laboratory have been found, for example, plasma processing is used in the semiconductor manufacturing industry (Ekeberg 2003), and dust charging can be applied in the electrostatic precipitation, separation and spraying as well as in the sterilization and electrophoresis

† Email address for correspondence: tian_bupt@163.com

https://doi.org/10.1017/S0022377814000543 Published online by Cambridge University Press

of biological materials (Kuznetsov et al. 1986; Li and Sattinger 1999; Liu et al. 2013). Experimental observations and numerical simulations on the DIA solitons in the dusty plasmas have been made (Kuznetsov et al. 1986; Li and Sattinger 1999; Liu et al. 2013; Dubinov and Kolotkov 2012; El-Tantawy et al. 2014; Husko et al. 2013; Kumar et al. 2013). Those investigations have made the existence of steady-state nonlinear structures in the dusty plasmas possible (Husko et al. 2013; Kumar et al. 2013), and revealed that the studies on the solitons, especially the soliton propagation and interaction between two solitons, can help people know the mechanism of dusty-plasma interaction (Kuznetsov et al. 1986; Li and Sattinger 1999; Liu et al. 2013; Dubinov and Kolotkov 2012; El-Tantawy et al. 2014; Husko et al. 2013; Kumar et al. 2013). In addition, solitons possess the infinite conservation laws and can form a nonlinear basis set for people to study the nonlinear problems (Ekeberg 2003). Analytical and numerical studies on the solitons in the plasmas have been given (Sun et al. 2011a; Sun et al. 2011b; Sun et al. 2013; Shen et al. 2014; Zuo et al. 2014a; Zuo et al. 2014b).

With both the azimuthal and height perturbations considered, for the cosmic DIA waves in a cosmic unmagnetized dusty plasma, people have worked out a generic variable-coefficient model as (Gao and Tian 2006)

$$\frac{\partial n_i}{\partial T}+\frac{1}{\gamma}\frac{\partial(\gamma n_i u_i)}{\partial \gamma}+\frac{1}{\gamma}\frac{\partial(n_i u_i)}{\partial \vartheta}+\frac{\partial(n_i w_i)}{\partial Z}=0, \tag{1a}$$

$$\frac{\partial u_i}{\partial T}+u_i\frac{\partial u_i}{\partial \gamma}+\frac{v_i}{\gamma}\frac{\partial u_i}{\partial \vartheta}+w_i\frac{\partial u_i}{\partial Z}+\frac{u_i v_i}{\gamma}=\frac{\partial \Phi}{\partial \gamma}, \tag{1b}$$

$$\frac{\partial v_i}{\partial T}+u_i\frac{\partial v_i}{\partial \gamma}+\frac{v_i}{\gamma}\frac{\partial v_i}{\partial \vartheta}+w_i\frac{\partial v_i}{\partial Z}+\frac{u_i v_i}{\gamma}=-\frac{1}{\gamma}\frac{\partial \Phi}{\partial \vartheta}, \tag{1c}$$

$$\frac{\partial w_i}{\partial T}+u_i\frac{\partial w_i}{\partial \gamma}+\frac{v_i}{\gamma}\frac{\partial w_i}{\partial \vartheta}+w_i\frac{\partial w_i}{\partial Z}=-\frac{\partial \Phi}{\partial Z}, \tag{1d}$$

$$\frac{1}{\gamma}\frac{\partial}{\partial \gamma}\left(\gamma\frac{\partial \Phi}{\partial \gamma}\right)+\frac{1}{\gamma^2}\frac{\partial^2 \Phi}{\partial \vartheta^2}+\frac{\partial^2 \Phi}{\partial Z^2}=\mu e^{\Phi}-n_i+(1-\mu), \tag{1e}$$

where n_i is the ion number density, T, γ, ϑ and Z represent the time, radial, azimuthal and height coordinates, u_i, v_i and w_i are the ion fluid velocities in the γ, ϑ and Z directions, respectively, Φ is the electrostatic wave potential normalized by $\kappa_B T_e/e$, e, T_e and κ_B are the magnitude of electronic charge, electron temperature and Boltzmann's constant, respectively, and $\mu=n_{e0}/n_{i0}$, with n_{e0} and n_{i0} being the equilibrium electron and ion densities, respectively.

Through the reductive perturbation, Φ can be expanded in a power series of a small parameter χ as $\Phi=\chi\Phi^{(1)}+\chi^2\Phi^{(2)}+\cdots$, with χ being the formal parameter. Via the independent variable transformations,

$$x=\chi^{\frac{1}{2}}(\gamma-cT),\quad y=\chi^{-\frac{1}{2}}\vartheta,\quad z=\chi Z,\quad t=\chi^{\frac{3}{2}}T, \tag{2}$$

where c is a real constant, System (1) can be reduced to a $(3+1)$-dimensional generalized Johnson model for the first approximation of the electrostatic wave potential $\phi=\Phi^{(1)}$ as follows (Gao and Tian 2006):

$$\phi_{xt}+A(\phi\phi_x)_x+B\phi_{xxxx}+\frac{\phi_x}{2t}+\frac{\sqrt{\mu}}{2t^2}\phi_{yy}+\frac{1}{2\sqrt{\mu}}\phi_{zz}=0, \tag{3}$$

with

$$A=\frac{3\mu-1}{2\sqrt{\mu}},\quad B=\frac{1}{2\mu^{\frac{3}{2}}}. \tag{4}$$

https://doi.org/10.1017/S0022377814000543 Published online by Cambridge University Press

Equation (3) can be used to describe the propagation of the DIA waves in a cosmic unmagnetized dusty plasma (Xue 2003; Gao and Tian 2006). It has been found that the preconditions for equation (3) and its nebulons can be met by such plasma systems as the supernova shells and Saturn's F-ring (Shukla and Mamun 2002). Such preconditions require that the system be a fully-ionized, gravity-effect-neglected, weakly-coupled, three-component dusty plasma (Mendis 2002; Shukla and Mamun 2002; Choi et al. 2005; Moslem 2006).

Some studies have been conducted on equation (3). Supernova-shell-typed expanding bright (3 + 1)-dimensional Johnson nebulons and Saturn-F-ring-type expanding dark (3 + 1)-dimensional Johnson nebulons have been discussed (Gao and Tian 2006). Existence and stability of the approximate soliton solutions of (3) have been given numerically (Xue 2003). This paper will consider the soliton solutions of (3), involving the soliton propagation and interaction, which have not been obtained in the early literatures.

Considering the coercive perturbation $g(t)$ on (3), we will also study the model (Narayanan et al. 2012)

$$\phi_{xt} + A(\phi\phi_x)_x + B\phi_{xxxx} + \frac{\phi_x}{2t} + \frac{\sqrt{\mu}}{2t^2}\phi_{yy} + \frac{1}{2\sqrt{\mu}}\phi_{zz} = g(t), \tag{5}$$

which can be found in an unmagnetized dusty plasma when the electron temperature T_e has been decreased below the Curie temperature (T_C) (Narayanan et al. 2012). Numerical studies have been employed on equation (5), with the nonlinear behavior agreeing with that measured in the experiments (Narayanan et al. 2012).

To give some insights on the nonlinear behavior of (5), we will study it from another point of view with the help of some qualitative and quantitative methods: Literatures have shown that the chaos is a sustained and disorderly-looking long-term evolution that satisfies certain criteria and occurs in a deterministic nonlinear system (Williams 1997; Hirsch et al. 2004). Numerical and analytic studies have revealed the existence of chaotic motions of the systems with the external period perturbations (Moon 1990; Scharf and Bishop 1992; Sreelatha and Joseph 1998; Blyuss 2000). Period-doubling and quasi-period-doubling sequences have been investigated as the routes to the chaos (Nokazi and Bekki 1983; Zheng et al. 1989; Williams 1997).

In this paper, with the Hirota method and symbolic computation (Hirota 2004; Hirota 1971), we will obtain the soliton solutions of (3) in Sec. 2. Then the propagation of one soliton and two kinds of interactions between the two solitons will be pictured in Sec. 3. With the phase-plane analysis, Hamiltonian integrability and periodicity of (3) will be given in Sec. 4. In Sec. 5, we will study (5) numerically with two kinds of the chaotic motions and periodic motion obtained. With the power spectra and largest Lyapunov exponents given, we will corroborate that such motions are indeed chaotic or periodic. Finally, our conclusions will be presented in Sec. 6.

2. Soliton solutions of (3)

2.1. *Bilinear form*

Setting $\phi = e^{-\frac{1}{2}\ln|t|}\varphi$, we can rewrite (3) as

$$\varphi_{xt} + A(\varphi\varphi_x)_x + B\varphi_{xxxx} + \frac{\varphi_x}{2t} + \frac{\sqrt{\mu}}{2t^2}\varphi_{yy} + \frac{1}{2\sqrt{\mu}}\varphi_{zz} = 0, \tag{6}$$

https://doi.org/10.1017/S0022377814000543 Published online by Cambridge University Press

where φ is a real function of x, y, z and t. Through the dependent variable transformation,

$$\varphi = \frac{6B}{A}(\ln f)_{xx}, \tag{7}$$

we can obtain the bilinear form of (6) as

$$\left(D_x D_t + B D_x^4 + \frac{\sqrt{\mu}}{2t^2} D_y^2 + \frac{1}{2\sqrt{\mu}} D_z^2\right) f \cdot f = 0, \tag{8}$$

where $f = f(x, y, z, t)$ is the real function to be determined, while D_x, D_y, D_z and D_t are the bilinear operators (Hirota 2004; Hirota 1971) defined by

$$D_{x_1}^{n_1} D_{x_2}^{n_2} F \cdot G = [\partial(x_1 - x_1')]^{n_1} [\partial(x_2 - x_2')]^{n_2} F(x_1, x_2) G(x_1', x_2')|_{x_1'=x_1, x_2'=x_2},$$

where n_j's ($j = 1, 2$) are both the positive integers, x_1' and x_2' are both the formal variables, F is the real function about the variables x_1 and x_2, and G is the real one about the formal variables x_1' and x_2'.

2.2. *Soliton solutions of (3)*

To construct the soliton solutions of (3), we expand f in the power series of a small parameter ϵ as

$$f = 1 + \epsilon f_1 + \epsilon^2 f_2 + \cdots, \tag{9}$$

where f_j's ($j = 1, 2, \cdots$) are all the real functions to be determined. Substituting Expansion (9) into Bilinear Form (8) and equating the coefficients of the same powers of ϵ to zero yield the recursion relations for f_j's ($j = 1, 2, \ldots$).

Truncating Expansion (9) as

$$f = 1 + \epsilon f_1 \tag{10}$$

and substituting Expression (10) into Bilinear Form (8), we can derive

$$f_1 = e^{\theta}, \quad \theta = kx + py + qz + w(t),$$

with k, p and q being all the real constants, and $w(t)$ being a real function. Thus, the constraints on the parameters can be obtained as

$$w(t) = \frac{-2Bk^4\sqrt{\mu}t^2 + \mu p^2 - q^2 t^2}{2k\sqrt{\mu}t}. \tag{11}$$

Without loss of generality, we set $\epsilon = 1$ and the one-soliton solutions of (3) can be expressed as

$$\phi = \frac{6\mu^2}{3\mu - 1} e^{-\frac{1}{2}\ln|t|}[\ln(1 + f_1)]_{xx} = \frac{3\mu^2 k}{3\mu - 1} e^{-\frac{1}{2}\ln t} \operatorname{sech}^2\left(\frac{\theta}{2}\right). \tag{12}$$

Similarly, if we truncate Expansion (9) as

$$f = 1 + \epsilon f_1 + \epsilon^2 f_2, \tag{13}$$

substitute Expression (13) into Bilinear Form (8), and then collect the terms with the same power of ϵ, we have

$$f_1 = e^{\theta_1} + e^{\theta_2}, \quad f_2 = \beta e^{\theta_1 + \theta_2}$$

with

$$\theta_1 = k_1 x + p_1 y + q_1 z + w_1(t), \quad \theta_2 = k_2 x + p_2 y + q_2 z + w_2(t),$$

https://doi.org/10.1017/S0022377814000543 Published online by Cambridge University Press

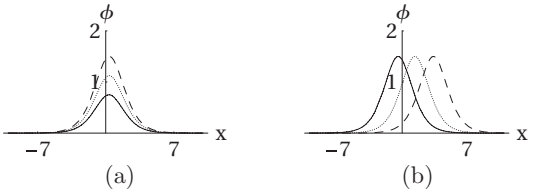


FIGURE 1. Effects of the equilibrium electron and ion densities on the one soliton via Solutions (12) with $z= y= 1$ at $t = 0.5$. Parameters are $k = 1$, $p= 0.5$, $q= 0.2$, (a) the solid line remarks the case $\mu = 4$ and $B = 0.0625$; the dotted line, $\mu = 3$ and $B = 0.096$; the dashed line, $\mu = 2$ and $B = 0.18$; (b) the solid line remarks the case $\mu = 2$ and $B = 0.18$; the dotted line, $\mu = 1.1$ and $B = 0.48$; the dashed line, $\mu = 0.5$ and $B = 1.43$.

and β being a real constant. So the constraints on the coefficients can be obtained as

$$w_1(t) = \frac{-2Bk_1^4\sqrt{\mu}t^2 + \mu p_1^2 - q_1^2t^2}{2k_1\sqrt{\mu}t}, \quad w_2(t) = \frac{-2Bk_2^4\sqrt{\mu}t^2 + \mu p_2^2 - q_2^2t^2}{2k_2\sqrt{\mu}t}, \tag{14a}$$

$$\begin{aligned}\beta = 1 - 24Bk_1^3k_2^3\sqrt{\mu}t^2/\big[&6Bk_2^2k_1^4\sqrt{\mu}t^2 + 12Bk_2^3k_1^3\sqrt{\mu}t^2 - k_2^2\left(\mu p_1^2 + q_1^2t^2\right)\\ &+ k_1^2\left(6Bk_2^4\sqrt{\mu}t^2 - \mu p_2^2 - q_2^2t^2\right) + 2k_2k_1\left(\mu p_1p_2 + q_1q_2t^2\right)\big].\end{aligned} \tag{14b}$$

Setting $\epsilon = 1$, we can derive the two-soliton solutions of (3) as

$$\phi = \frac{6\mu^2}{3\mu - 1}e^{-\frac{1}{2}\ln|t|}[\ln(1 + f_1 + f_2)]_{xx}. \tag{15}$$

3. Discussions on the solitons

For the DIA solitons in the dusty plasmas, several experiments have been conducted, and specific conditions for such solitons have been listed (Mendis 2002; Dubinov and Kolotkov 2012; El-Tantawy et al. 2014; Husko et al. 2013; Kumar et al. 2013), such as Tables 1 and 2 in Mendis (2002). It is found that the solitons can be observed with the balance between the nonlinearity and dispersion, and the experimentally recorded soliton profiles keep unchanged during the propagation Mendis (2002). In this part, we want to display the soliton propagation according to the analytic expressions.

Based on Solutions (12), we will show the propagation of the one soliton in Fig. 1, from which we see that the amplitude, velocity and width of the bell-shaped soliton keep invariable during the propagation. Figure 1(a) shows that the amplitude of the one soliton is inversely related to the value of $\mu = n_{e0}/n_{i0}$. However, from Fig. 1(b), we find that the amplitude of the one soliton does not increase at all even though μ keeps decreasing when $\mu \leqslant 2$. Therefore, amplitude of the one soliton will reach the maximum when the equilibrium electron and ion densities take certain values which corresponds with $\mu = 2$. For the supernova shells or other similar dusty plasmas, Fig. 1 helps us to know the propagation of electrostatic wave potential Φ. Through the discussions on the one soliton, we can obtain the effects of equilibrium electron density n_{e0} and ion density n_{i0} on such Φ.

Two kinds of interactions between the two bell-shaped solitons are shown in Fig. 2. The soliton with the faster velocity surpasses the slower in the same direction, which means that the overtaking interaction occurs in Fig. 2(a). Two solitons move with certain amplitudes, velocities, widths and pass through each other unaffectedly with different directions, which presents the head-on interaction in Fig. 2(b). From Fig. 2, we can see that two kinds of interactions between the two solitons are both elastic.

https://doi.org/10.1017/S0022377814000543 Published online by Cambridge University Press

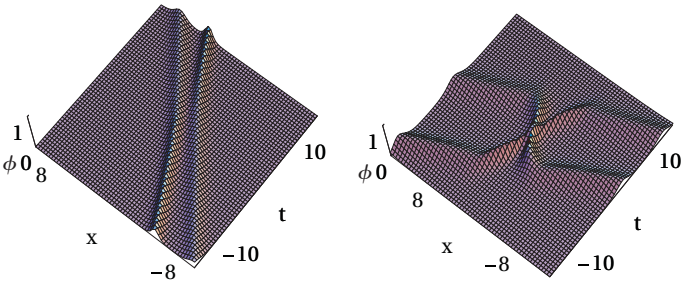


FIGURE 2. Interaction between the two solitons via Solutions (15) with $y = z = 1$ at $t = 1$. (a) Overtaking interaction is displayed when $k_1 = 0.8$, $k_2 = 1$, $\mu = 1$, $p_1 = 0.4$, $p_2 = 0.2$, $q_1 = 0.5$, $q_2 = 0.75$ and $B = 0.5$; (b) Head-on interaction is displayed when $k_1 = 0.8$, $k_2 = -0.5$, $\mu = 1$, $p_1 = 0.4$, $p_2 = -0.5$, $q_1 = 0.5$, $q_2 = -0.3$ and $B = 0.5$.

It has been investigated the studies on the soliton interaction can help us know the interaction between the dust and ambient plasma, which leads to the dust charging with consequences for both the dust and the plasma.

4. Phase-plane analysis on Eqs. (6)

Phase-plane analysis is a kind of qualitative analysis, which can help people to know some dynamic characteristics of the nonlinear evolution equations (Infeld and Rolands 1990; Yu et al. 2007). Setting $\phi(x, y, z, t) = \psi(\xi)$ with $\xi = r_1 x + r_2 y + r_3 z - r_4(t)$, where r_1, r_2 and r_3 are all real constants, and $r_4(t)$ is a real function, and substituting $\psi(\xi)$ into (3), we have

$$\psi_{\xi\xi\xi} + \alpha_1 \psi_\xi + \alpha_2 \psi + \alpha_3 \psi \psi_\xi = 0, \tag{16}$$

with

$$\alpha_1 = \frac{2\sqrt{\mu} r_1 r_4'(t) t^2 + \mu r_2^2 + r_3^2 t^2}{2\sqrt{\mu} B r_3^2 t^2}, \quad \alpha_2 = \frac{1}{2tBr_1^3}, \quad \alpha_3 = \frac{A}{Br_1^2}, \tag{17}$$

where $r_4'(t) = dr_4(t)/dt$, and α_1 is a real function of t. Expression (16) is equivalent to the three-dimensional planar dynamic system (Yu et al. 2007) as follows ($X \equiv \psi$, $Y \equiv \psi_\xi$, $Z \equiv \psi_{\xi\xi}$):

$$X_\xi = Y, \quad Y_\xi = Z, \quad Z_\xi = -\alpha_1 Y - \alpha_2 X - \alpha_3 XY. \tag{18}$$

Based on (Yu et al. 2007; Infeld and Rolands 1990), System (18) is Hamilton integrable when it is undamped, i.e., $\alpha_1 = 0$, and via the Melnikov procedure (Infeld and Rolands 1990), we can get the Hamiltonian as

$$H(X, Y, Z) = \frac{1}{2}Z^2 + \frac{1}{2}Y^2 - \frac{1}{2}\alpha_2 X^2 - \frac{1}{2}\alpha_3 X^2 Y. \tag{19}$$

Traveling-wave solutions of (3) can be determined by the phase orbits which can be defined by the vector fields (X,Y,Z) of System (18).

A closed curve, which can be used to represent the phase projection of System (18) when $\alpha_1 = 0$, is seen in Fig. 3(a), indicating that there is a central point in this case. When $\alpha_1 \neq 0$, the phase projection of System (18) is displayed in Fig. 4(a), in which we can see a stable focal point. To investigate if those oscillations are periodic, we

https://doi.org/10.1017/S0022377814000543 Published online by Cambridge University Press

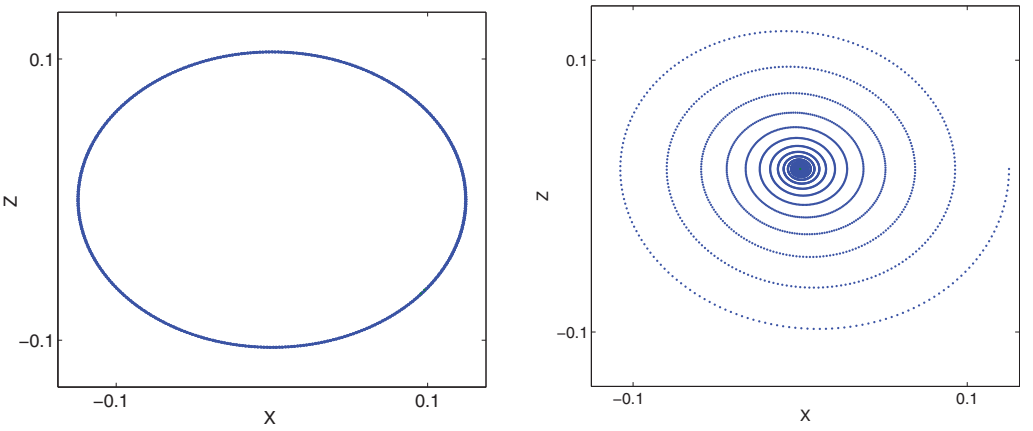


FIGURE 3. (a) Phase projection of System (18) with $\alpha_1=0$, $\alpha_2=\frac{1}{2t}$, $\alpha_3 = 0.5$. (b) Power spectra for the solutions of System (18) which correspond with Fig. 3(a).

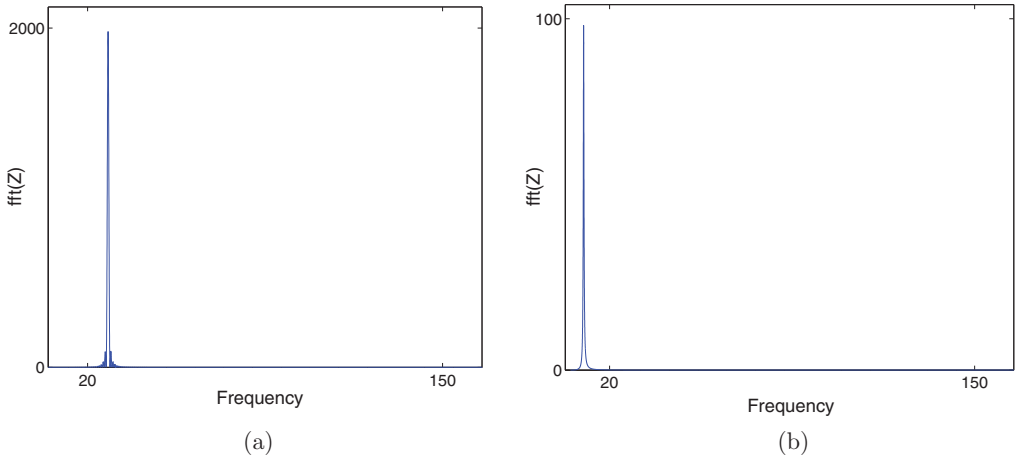


FIGURE 4. (a) Phase projection of System (18) with $\alpha_1=\frac{0.3t^2+2}{0.1t^2}$, $\alpha_2 = \frac{1}{2t}$, $\alpha_3 = 0.5$; (b) Power spectra for the solutions of System (18) which correspond with Fig. 4(a).

calculate their power spectra in Figs. 3(b) and 4(b) via spectral analysis. Since there only exists one frequency in the two figures, so periodicity of Z is displayed. Hereby, the frequency refers to the number of occurrences of a repeating event per unit time and it is the reciprocal of the periodicity (Infeld and Rolands 1990). In Fig. 3(b) and 4(b), the abscissa represents the frequency of Z under certain conditions, while the ordinate $fft(Z)$ represents the fast Fourier transform (FFT) of Z†.

† FFT is a method for computing the discrete Fourier transform (DFT) with a reduction in computer time (Bergland 1969; Stoica and Moses 1997). With a time series having N samples $(Z_0, \ldots, Z_{N-1})$, DFT of Z can be given as

$$A_j = \sum_{n=0}^{N-1} Z_n W_N^{nj}, \quad W_N = e^{-\frac{2\pi i}{N}}, \quad j = 0, 1, \ldots, N-1, \tag{20}$$

https://doi.org/10.1017/S0022377814000543 Published online by Cambridge University Press

5. Chaotic and periodic motions of (5)

In this section, with the help of phase-plane analysis and spectral analysis, we will exhibit the quasi-periodic or chaotic oscillations in a cosmic unmagnetized dusty plasma described by (5). Based on the numerical results from such methods, we aim to illustrate that (5) may give rise to two kinds of chaotic motions, i.e., the weak and developed chaos, and then we will investigate the main cause for the difference between the two chaotic motions. Moreover, we will find that (5) can turn into the periodic state in response to the appropriate strength of the external perturbations, and the effect of the damped term on such a periodic state. Note that the concept of "quasi-periodic" can be found (Corsi and Gentile 2012; Jitomirskaya and Marx 2012; Sahu et al. 2012).

5.1. *Phase-plane analysis on (5)*

First, we will conduct the phase-plane analysis on (5). Setting $\phi(x, y, z, t) = \psi(\xi)$ with $\xi = r_1 x + r_2 y + r_3 z - r_4(t)$, and substituting $\psi(\xi)$ into (5), we can derive

$$\psi_{\xi\xi\xi} + l_1\psi_\xi + l_2\psi + l_3\psi\psi_\xi = l_4 g(t)\xi, \tag{23}$$

with

$$l_1 = \frac{\mu r_2^2 + 2r_3^2 t^2 - 2t^2\sqrt{\mu} r_1 r_4'(t)}{2Br_1^4 t^2}, \quad l_2 = \frac{1}{2tBr_1^3}, \quad l_3 = \frac{A}{Br_1^2}, \quad l_4 = \frac{1}{Br_1^4}. \tag{24}$$

Therefore, System (23) can be rewritten as the "four-dimensional" planar dynamic system as follows [$X \equiv \psi$, $Y \equiv \psi_\xi$, $Z \equiv \psi_{\xi\xi}$, $G \equiv g(t)\xi$]:

$$X_\xi = Y, \quad Y_\xi = Z, \quad Z_\xi = -l_1 Y - l_2 X - l_3 XY + l_4 G, \quad G_\xi = g(t). \tag{25}$$

where the absolute values of $g(t)$, l_1 and l_3 can be used to measure the strength of the external perturbation, damped term and nonlinear term, respectively.

5.2. *Two kinds of chaotic motions of (5)*

Based on System (25), people might ask: Can any chaotic motions be expected when the strength of external perturbation varies? Are there any differences among the chaos? Considering the problems above, we will study System (25) numerically, then we will illustrate the occurrence of dynamic chaos or quasi-periodic behavior in (5).

Figure 5(a) displays that Z of System (25) has two different frequencies, one of which is produced by the external perturbation $g(t)$. Comparing Fig. 5(a) with Fig. 3(b), we can find that the frequency of the external perturbation is superimposed on the

where N is an even constant. Z_n can be divided into two parts, $Z_{1,n}$ and $Z_{2,n}$, with $Z_{1,n}$ being composed of the even-number points, while $Z_{2,n}$, the odd-number points. $Z_{1,n}$ and $Z_{2,n}$ are the sequences of $N/2$ points each, and the DFT of them can be defined as

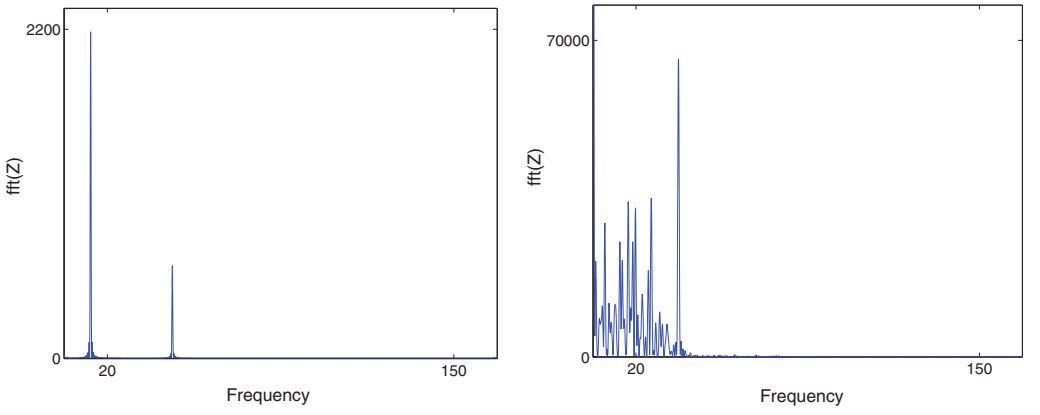
$$B_j = \sum_{n=0}^{N/2-1} Z_n W_N^{nj}, \quad C_j = \sum_{n=0}^{N/2} Z_n W_N^{nj}, \quad j = 0, 1, \ldots, N/2. \tag{21}$$

Therefore, the FFT of Z can be given as

$$A_j = B_j + W_N^j C_j, \quad A_{j+N/2} = B_j + W_N^j C_j, \quad 0 \leqslant j < N/2 - 1. \tag{22}$$

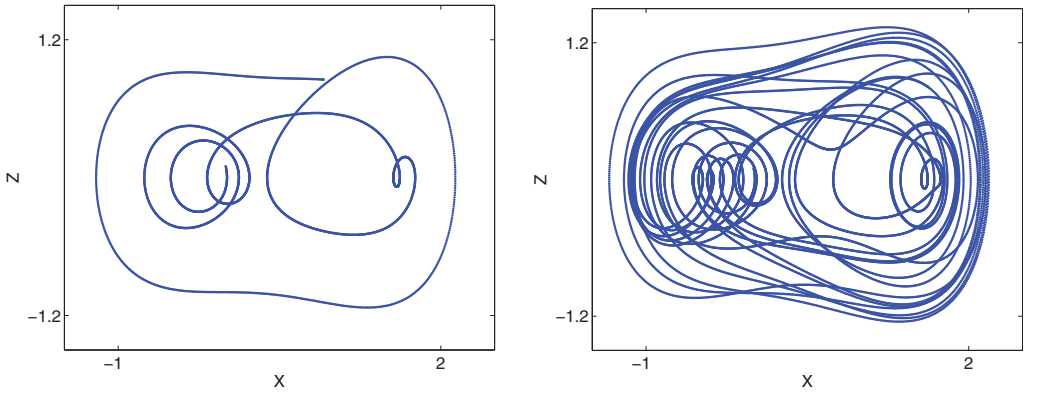
Note that N^2 multiplications and N^2 additions are required in the DFT, but only $N/2\log_2 N$ multiplications and $N\log_2 N$ additions in the FFT with N samples in numerical simulations (Bergland 1969; Stoica and Moses 1997).

https://doi.org/10.1017/S0022377814000543 Published online by Cambridge University Press



(a) (b)

FIGURE 5. Power spectra of the solutions produced by System (25). Parameters are: (a) $l_1 = 0.4$, $l_2 = 0.5$, $l_3 = 2.4$, $l_4 = 1$ and $g(t) = 0.05 \sin t$; (b) $l_1 = 0.4$, $l_2 = 0.05$, $l_3 = 0.426$, $l_4 = 1$ and $g(t) = 2 \sin t$.



(a) (b)

FIGURE 6. Phase projection of the developed chaotic motion of System (25) with $l_1 = 0.4$, $l_2 = 0.05$, $l_3 = 0.426$, $l_4 = 1$ and $g(t) = 2\sin t$, (a) from $t = 0.1$ to $t = 15.4$; (b) from $t = 0.1$ to $t = 150$.

original frequency of System (18) when $l_3 \ll |g(t)|$. It is called the "weak chaos" since there only exists a small chaotic deviation from the periodic solutions (Malkov 1996; Laptyeva et al. 2010; Basko 2011; Mulansky 2011). Now we can see that the small chaotic deviation occurs because of the superimposition of the two frequencies.

However, another chaotic motion occurs in (5), as shown in Fig. 5(b). Comparing Fig. 5(b) with 3(b), we see that the original frequency of System (18) is broken. Note that the maximum of intensity shown in Fig. 5(b) is bigger than that in Fig. 5(a), and no periodicity can be seen in Fig. 5(b). Refs. (Ryskin and Titov 2011; Lalescu et al. 2013) have defined this motion as the "developed chaos" in which the solutions ignore the driver periods and represent a random sequence of uncorrelated shocks.

To find out the final states of the two chaotic motions, we would like to display the phase projections of System (25), as shown in Figs. 6–7. Note that different values of $g(t)$ and l_3 are used in Figs. 6–7.

https://doi.org/10.1017/S0022377814000543 Published online by Cambridge University Press

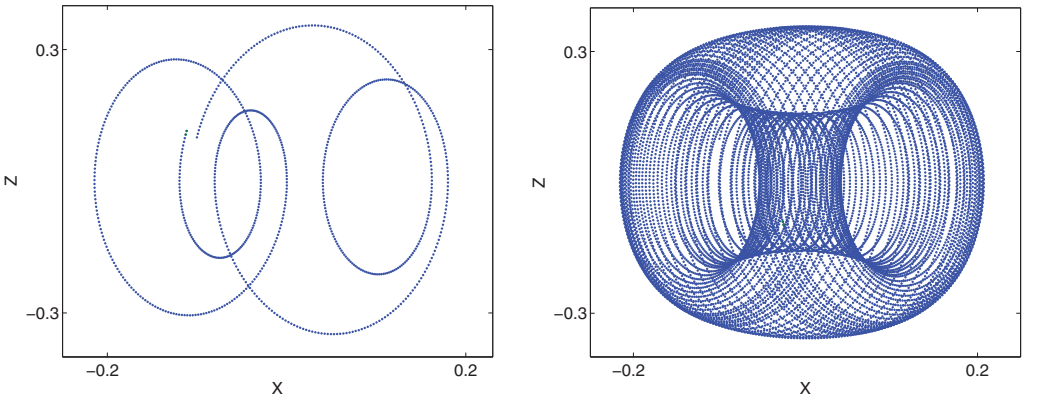


FIGURE 7. Phase projection of the weak chaotic motion of System (25) with $l_1 = 0.4$, $l_2 = 0.05$, $l_3 = 2.4$, $l_4 = 1$ and $g(t) = 0.05\sin t$, (a) from $t = 0.1$ to $t = 5.97$; (b) from $t = 0.1$ to $t = 150$.

As expected, the chaotic behavior shown in Figs. 6–7 is consistent with the spectra which are displayed in Fig. 5.

No periodicity can be found in Fig. 6 and the developed chaos occurs there. Although Z in Fig. 6 is convergent, the value and propagation of Z cannot be predicted within a certain range yet. Thus, we want to find a way, such as the adjustment of the values of l_3 and $g(t)$, to weaken the chaotic motions shown in Fig. 6, and then propagation of the solutions of System (25) can be predicted.

Weak chaos occurs in Fig. 7. One period of the quasi-periodic state is shown in Fig. 7(a), i.e., from $t = 0.1$ to $t = 5.97$. With time evolution, System (25) turns into the weak chaotic states, as displayed in Fig. 7(b). Comparing Figs. 6 and 7, we can find that the propagation of Z can be predicted in the case of weak chaos.

Further, we want to find the cause for the difference between the two chaotic motions which are respectively displayed in Figs. 6 and 7. In Fig. 6, the maximum value of $g(t)$ is 2, but $l_3 \ll 2$. However, in Fig. 7, the maximum value of $g(t)$ is 0.05, and $l_3 \gg 0.05$. It means that the solutions of System (25) will "ignore" the periodicity of System (18) when the strength of $g(t)$ is much stronger than that of l_3, so System (18) might turn into the developed chaos; otherwise, weak chaos occurs. Based on Expressions (4) and (24), we can find that when $\mu < 1$, i.e., $n_{e0} < n_{i0}$, l_3 is inversely related to μ. Thus, if $n_{e0} < n_{i0}$, the decrease of n_{i0} can weaken the chaotic motions, or the increase of n_{i0} can weaken the chaotic motions.

To corroborate that the behavior in Figs. 6 and 7 is indeed chaotic, we will investigate the largest Lyapunov exponents (Beiglböck et al. 2000; Hirsch et al. 2004) of external perturbation $g(t)$ with different values of nonlinear term l_3, as shown in Fig. 8.

Dynamic behavior of System (25) varying with $g(t)$ is displayed in Fig. 8(a). We find that System (25) can give rise to the periodic motions when $0.05 < |g(t)| < 0.15$ or $0.26 < |g(t)| < 0.28$, while chaotic motions occur when $0.03 < |g(t)| < 0.05$ or $0.15 < |g(t)| < 0.26$ or $0.26 < |g(t)| < 0.6$. Weak chaos may occurs at the critical points $|g(t)| = 0.03, 0.05, 0.15, 0.26, 0.28$. When l_3 decreases, different dynamic behavior of System (25) varying with $g(t)$ is displayed in Fig. 8(b). Note that System (25) turns into the periodic states when $0.25 < |g(t)| < 1.6$, while it is chaotic when $0.21 < |g(t)| < 0.25$ or $1.6 < |g(t)| < 3$. As expected, the largest Lyapunov exponents

https://doi.org/10.1017/S0022377814000543 Published online by Cambridge University Press

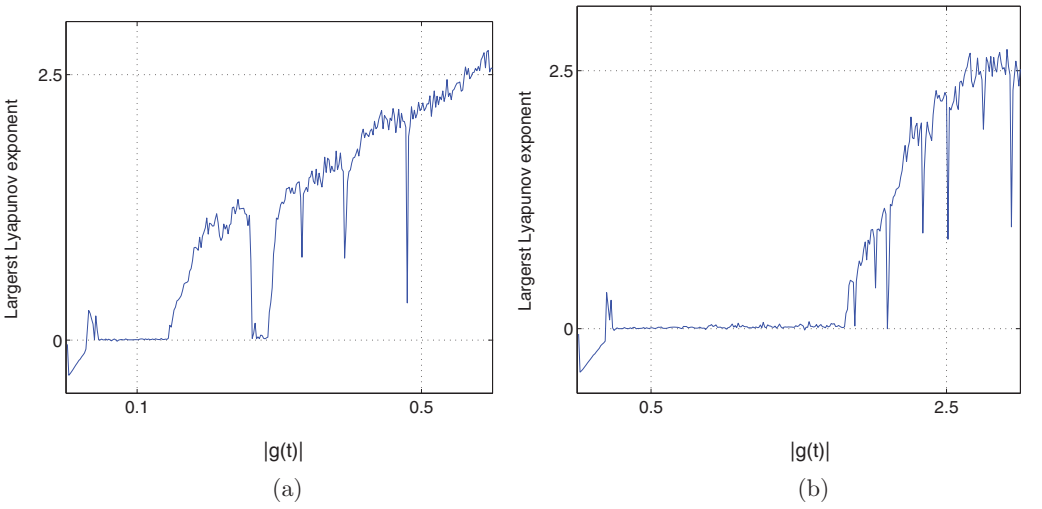


FIGURE 8. Largest Lyapunov exponents when the external perturbation $g(t)$ is the bifurcation parameter and different nonlinear term l_3, while $l_1 = 0.4$, $l_2 = 0.05$, $l_4 = 1$; (a) $l_3 = 2.4$; (b) $l_3 = 0.426$.

in Figs. 8(a) and 8(b) are consistent with the motions shown in Figs. 6 and 7, respectively.

5.3. *Periodic motions of (5)*

Next, two more questions will be asked: Can the periodic state be expected when there exists a balance between the external perturbation $g(t)$ and nonlinear term l_3? Is there any difference among the periodic states at the different strength of the damped term? We will work on them based on the phase projections and power spectra.

Two different periodic motions are displayed in Fig. 8, and the one period of two periodic motions is displayed in Fig. 8. Comparing Fig. 8(a) with 8(b), we can find that the range of Z and one-period time both decrease with the damped term l_1 increased. Since l_1 is positively related to n_{i0} when $n_{e0} < 4n_{i0}$, or inversely related to n_{i0} when $n_{e0} > 4n_{i0}$. Thus, the range of Z and one-period time are both inversely related to n_{i0} when $n_{e0} < 4n_{i0}$; otherwise, they are positively related to n_{i0}.

To corroborate that the behavior shown in Fig. 9 is indeed periodic, we calculate the power spectra corresponding to the solutions of System (25), as shown in Fig. 10. Since Z in Fig. 9 only has the single frequency, Fig. 10 may corroborate that the motions, as exhibited in Fig. 9, are indeed periodic. The difference between Fig. 10(a) and 10(b) is the value of l_1 and range of Z. We can find that the range of Z may decrease with the increase of l_1. As expected, the spectra exhibited in Fig. 10 are consistent with those of the periodic states displayed in Fig. 9.

6. Conclusions

In this paper, we have considered the (3+1)-dimensional generalized Johnson model, i.e., (3), which can be used to describe the DIA waves in a cosmic unmagnetized dusty plasma, and its perturbed form, i.e., (5), which can be found in an unmagnetized dusty plasma when the electron temperature T_e has been decreased below the Curie temperature. Results of this paper can be summarized as below:

https://doi.org/10.1017/S0022377814000543 Published online by Cambridge University Press

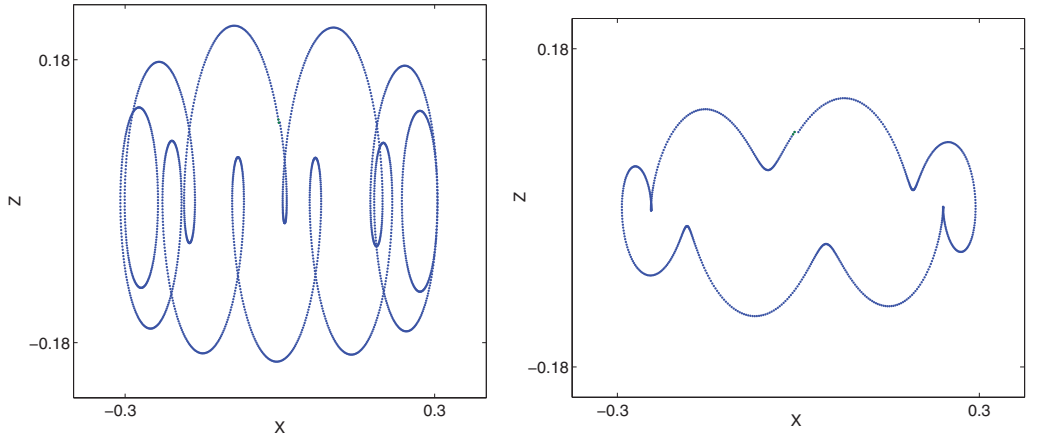


FIGURE 9. Phase projection of the periodic chaotic motion of System (25) with $l_2 = 0.5$, $l_3 = 2.4$, $l_4 = 0.1$ and $g(t) = 0.05\sin t$, (a) $l_1 = 0.2$ from $t = 0.1$ to $t = 20$; (b) $l_1 = 1$ from $t = 0.1$ to $t = 7.01$.

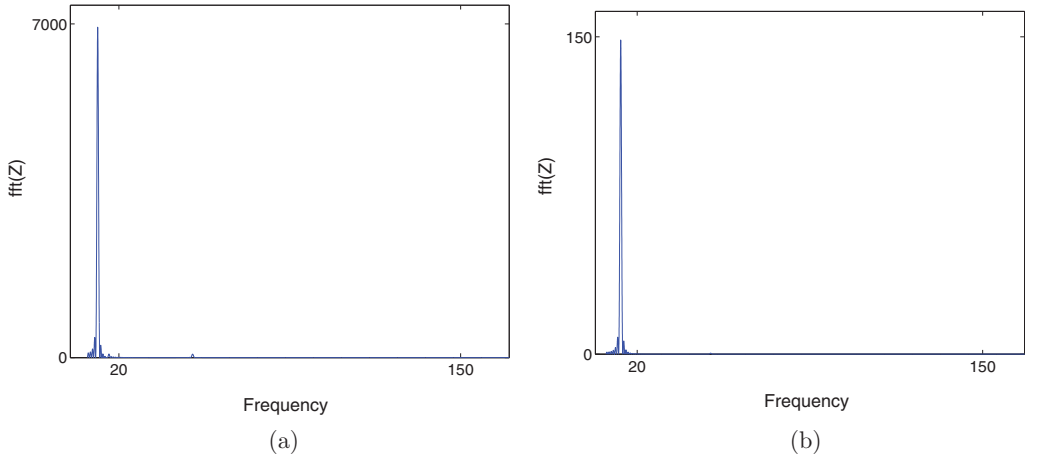


FIGURE 10. Power spectra of the solutions produced by System (25). Parameters are: $l_2 = 0.5$, $l_3 = 2.4$, $l_4 = 0.1$ and $g(t) = 0.05\sin t$, (a) $l_1 = 0.2$; (b) $l_1 = 1$.

• Bilinear Form (8) and Soliton Solutions (12) and (15) of (3) have been obtained with the help of Hirota method and symbolic computation.

• Propagation of the one soliton and interaction between the two solitons have been shown. Figure 1 has shown that the amplitude of the one soliton reaches the maximum when the equilibrium electron density n_{e0} and equilibrium ion density n_{i0} take certain values which correspond with $\mu = 2$. Two kinds of the interaction between the two solitons have been displayed in Fig. 2.

• Equation (3) has been reduced to the ordinary differential system, i.e., System (18), via the phase-plane analysis. Effect of the damped term l_1 has been investigated, i.e., central point has been shown in Fig. 3(a) if $l_1 = 0$, or focal point in Fig. 4(a). Periodicity of the two cases has been given in Figs. 3(b) and 4(b).

• For (5), two kinds of the power spectra have been given, as shown in Fig. 5, based on which the chaotic and periodic behavior has been given numerically.

https://doi.org/10.1017/S0022377814000543 Published online by Cambridge University Press

• Both the weak and developed chaotic motions have been displayed in Figs. 6 and 7, with different values of the external perturbation $g(t)$ and nonlinear term l_3 chosen. We have given a way to predict the chaos for the cosmic dust-ion-acoustic nebulons, which can be described by (5).

• Largest Lyapunov exponents with $g(t)$ being the bifurcation parameter have been displayed in Fig. 8. We have seen that (5) can indeed give rise to chaotic motions, and dynamic behavior of (5) varying with $g(t)$ changes with different values of l_3.

• Figure 9 has exhibited two kinds of the periodic motions with the different values of the damped term l_1 chosen. With the power spectra given in Fig. 10, we have corroborated that such motions are indeed periodic.

Acknowledgements

This work has been supported by the National Natural Science Foundation of China under Grant No. 11272023, by the Open Fund of State Key Laboratory of Information Photonics and Optical Communications (Beijing University of Posts and Telecommunications) under Grant No. IPOC2013B008, and by the Fundamental Research Funds for the Central Universities of China under Grant No. 2011BUPTYB02.

REFERENCES

Basko, D. M. 2011 *Ann. Phys.-Berlin* **326**, 1577.

Beiglböck, W., Eckmann, J. P., Grosse, H., Loss, M., Smirnov, S., Takhtajan, L. and Yngvason, J. 2000 *Concepts and Results in Chaotic Dynamics*. Berlin: Springer.

Bergland, G. D. 1969 *IEEE Spectrum* **6**, 228.

Blyuss, K. B. 2000 *Rep. Math. Phys.* **46**, 47.

Cao, H. J., Seoane, J. M. and Sanjuán, A. F. 2007 *Chaos Soliton. Fract.* **34**, 197.

Choi, C. R., Ryu, C. M., Lee, N. C., Lee, D. Y. and Kim, Y. 2005 *Phys. Plasmas* **12**, 072301.

Corsi, L. and Gentile, G. 2012 *Commun. Math. Phys.* **316**, 489.

Dubinov, A. E. and Kolotkov, D. Y. 2012 *High Energ. Chem.* **46**, 349.

Duha, S. S., Shikia, B. and Mamun, A. A. 2011 *Pramana-J. Phys.* **77**, 357.

Ekeberg, J. 2003 *Theory and Modelling of Magnetosonic Solitons in Space Plasma*. New York: Elsevier.

El-Tantawy, S. A., Moslem, W. M., Sabry, R., El-Labany, S. K., El-Metwally, M. and Schlickeiser, R. 2014 *Astrophys. Space Sci.* **350**, 175.

Fortov, V. E., Ivlev, A. V., Khrapak, S. A., Khrapak, A. G. and Morfill, G. E. 2005 *Phys. Rep.* **421**, 1.

Gao, Y. T. and Tian, B. 2006 *Phys. Plasmas* **13**, 120703.

Gao, Y. T. and Tian, B. 2006 *Phys. Lett.* A **349**, 314.

Gao, Y. T. and Tian, B. 2006 *Phys. Plasmas* **13**, 112901.

Higuchi, M. and Fukushima, K. 1998 *Chaos Solitons Fract.* **9**, 845.

Hirota, R. 2004 *The Direct Method in Soliton Theory*. Cambridge: Cambridge Univ. Press.

Hirota, R. 1971 *Phys. Rev. Lett.* **27**, 1192.

Hirsch, M. W., Smale, S. and Devaney, R. L. 2004 *Differential equations, Dynamical Systems, and an Introduction to Chaos*. New York: Elsevier.

Husko, C. A., Combrié, S., Cloman, P., Zhen, J. J., Rossi, A. D. and Wong, C. W. 2013 *Nature* **3**, 01100.

Infeld, E. and Rolands, G. 1990 *Nonlinear Waves, Soliton and Chaos*. Cambridge: Cambridge Univ. Press.

Jitomirskaya, S. and Marx, C. A. 2012 *Geom. Funct. Anal.* **22**, 1407.

Kumar, H., Malik, A. and Chand, F. 2013 *P. Indian AS-Math Sci.* **80**, 361.

Kuznetsov, E. A., Rubenchik, A. M. and Zakharov, V. E. 1986 *Phys. Rep.* **142**, 103.

https://doi.org/10.1017/S0022377814000543 Published online by Cambridge University Press

Lalescu, C. C., Meneveau, C. and Eyink, G. L. 2013 *Phys. Rev. Lett*. **110**, 084102.
Laptyeva, T. V., Bodyfelt, J. D., Krimer, D. O. and Flach, S. 2010 *Europhys. Lett*. **91**, 30001.
Li, Y. and Sattinger, D. H. 1999 *J. Math. Fluid Mech.* **1**, 117.
Liu, H. F., Wang, S. Q. and Yang, F. Z. 2013 *Astrophys. Space Sci.* **347**, 139.
Malkov, M. A. 1996 *Phys.* D **95**, 62.
Mendis, D. A. 2002 *Plasma Sources Sci. Tech.* **11**, A219.
Moon, H. T. 1990 *Phys. Rev. Lett*. **64**, 412.
Morfill, G. E., Tsytovich, V. N. and Thomas, H. 2003 *Plasma Phys. Rep*. **29**, 682.
Moslem, W. 2006 *Phys. Lett*. A **351**, 290.
Mulansky, M., Ahnert, K., Pikovsky, A. and Shepelyansky, D. L. 2011 *J. Stat. Phys.* **145**, 1256.
Narayanan, M., Tong, S., Ma, B. H., Liu, S. S. and Balachandran, U. 2012 *Phys. Plasmas*, **100**, 022907.
Nokazi, K. and Bekki, N. 1983 *Phys. Rev. Lett*. **50**, 1226.
Popel, S., Losseva, T., Golub, A., Merlino, R. and Andreev, S. 2005 *Contrib. Plasma Phys.* **45**, 461.
Ryskin, N. M. and Titov, V. N. 2011 *Tech. Phys.* **48**, 1170.
Sahu, B., Poria, S. and Roychoudhury, R. 2012 *Astrophys. Space Sci.* **341**, 567.
Sahu, B. and Roychoudhury, R. 2003 *Phys. Plasmas* **10**, 4162.
Scharf, R. and Bishop, A. R. 1992 *Phys. Rev.* A **46**, 6.
Shen, Y. J., Gao, Y. T., Zuo, D. W., Sun, Y. H., Feng, Y. J. and Xue L. 2014 *Phys. Rev. E* **89**, 062915.
Shen, Y. J., Gao, Y. T., Yu, X., Meng, G. Q. and Qin, Y. 2014 *Appl. Math. Comput*. **227**, 502.
Shukla, P. K. 2001 *Phys. Plasmas* **8**, 1791.
Shukla, P. K. and Mamun, A. A. 2002 *Introduction to Dusty Plasma Physics*. Bristol: IOP Pub.
Sreelatha, K. S. and Joseph, K. B. 1998 *Chaos Solitons Fract*. **9**, 1865.
Stoica, P. and Moses, R. L. 1997 *Introduction to Spectral Analysis*. New Jersey: Prentice Hall.
Sun, Z. Y., Gao, Y. T., Yu, X. and Liu, Y. 2011a *Europhys. Lett*. **93**, 40004.
Sun, Z. Y., Gao, Y. T., Liu, Y. and Yu, X. 2011b *Phys. Rev.* E **84**, 026606.
Sun, Z. Y., Gao, Y. T., Yu, X. and Liu, Y. 2013 *Phys. Lett*. A **377**, 3283.
Taylor, J. R. 1992 *Optical Solitons Theory and Experiment*. Cambridge: Cambridge Univ. Press.
Tian, B. and Gao, Y. T. 2005 *Phys. Plasmas* **12**, 054701.
Tian, B. and Gao, Y. T. 2005 *Phys. Plasmas* **12**, 070703.
Tian, B. and Gao, Y. T. 2005a *Phys. Lett*. A **340**, 449.
Tian, B. and Gao, Y. T. 2005b *Eur. Phys. J.* D **33**, 59.
Tsytovich, V. N., Morfill, G. E. and Thomas, H. 2002 *Plasma Phys. Rep*. **28**, 623.
Williams, G. P. 1997 *Chaos Theory Tamed*. Washington D. C.: Joseph Henry.
Xue, J. K. 2003 *Phys. Lett*. A **314**, 479.
Yang, J. K. and Kaup, D. J. 2000 *SIAM J. Appl. Math.* **60**, 967.
Yu, J., Zhang, W. J. and Gao, X. M. 2007 *Chaos Solitons Fract*. **33**, 1307.
Zheng, D. J., Yeh, W. J. and Symko, O. G. 1989 *Phys. Lett*. A **140**, 225.
Zuo, D. W., Gao, Y. T., Meng, G. Q., Shen, Y. J. and Yu, X. 2014a *Non. Dyn.* **75**, 701.
Zuo, D. W., Gao, Y. T., Sun, Y. H., Feng, Y. J. and Xue L. 2014b Z. Naturforsch. A, in press, DOI: 10.5560/ZNA.2014-0045.

https://doi.org/10.1017/S0022377814000543 Published online by Cambridge University Press